FAILURE ANALYSIS

Microstructural Analysis of Ethylene Furnace Steel Alloy Tubes

C.A. Loto, *Tshwane University of Technology, Pretoria, South Africa*

Several radiant tubes of an ethylene (C_2H_4) furnace at a petrochemical plant were analyzed after failure. Experimental results suggest that the failures were caused by exposure of the tubes to excessive temperature during service. It was recommended that the furnace temperature be closely controlled to avoid overheating the tubes.

Ethylene (C_2H_4) is produced by cracking ethane (C_2H_6) in pyrolysis furnaces. The process stream in a furnace consists of a mixture of steam and ethane, which is passed through a coil of reaction tubes externally heated to a temperature of 950 to 1,150 °C. The gas temperature is raised quickly and passed through the coil at a high velocity with a short residence time. The temperature in the reaction tube is ~850 °C. Cracking of ethane produces free carbon according to the reaction:

$$C_2H_4 \rightarrow CH_4 + C \quad (1)$$

Carbon produced by this reaction is deposited on the internal surface of the tube wall as adherent coke. The coke is removed by shutting off the hydrocarbon feed and passing air and steam through the coil. Such a process is called decoking. Frequent decoking accelerates the thermal damage of the tubes while less frequent decoking increases the rate of carburization attack.

The objective of this investigation was to evaluate the performance of the furnace tubes, which are of different material compositions, and draw conclusions as to their suitability in high-temperature service conditions. Similar work or closely related investigations[1-4] have been performed.

Experimental Procedures

The test materials were produced by Saudi Petrochemical Co. (SADAF), located at Al-Jubail Industrial City, and supplied by Saudi Basic Industries (SABIC). The nominal composition of the furnace tubes is:

- Tubes 1 and 2: 25Cr-20Ni-Fe (HK-40)
- Tubes 3 and 6: 25Cr-35Ni-Fe
- Tubes 7 and 9: 35Cr-48Ni-Fe

The as-received tube samples were visually inspected. The samples were cut to the appropriate size and mounted in cross-section for metallurgical evaluation in polished and etched condition. Scanning electron microscopy (SEM) was used

FIGURE 1

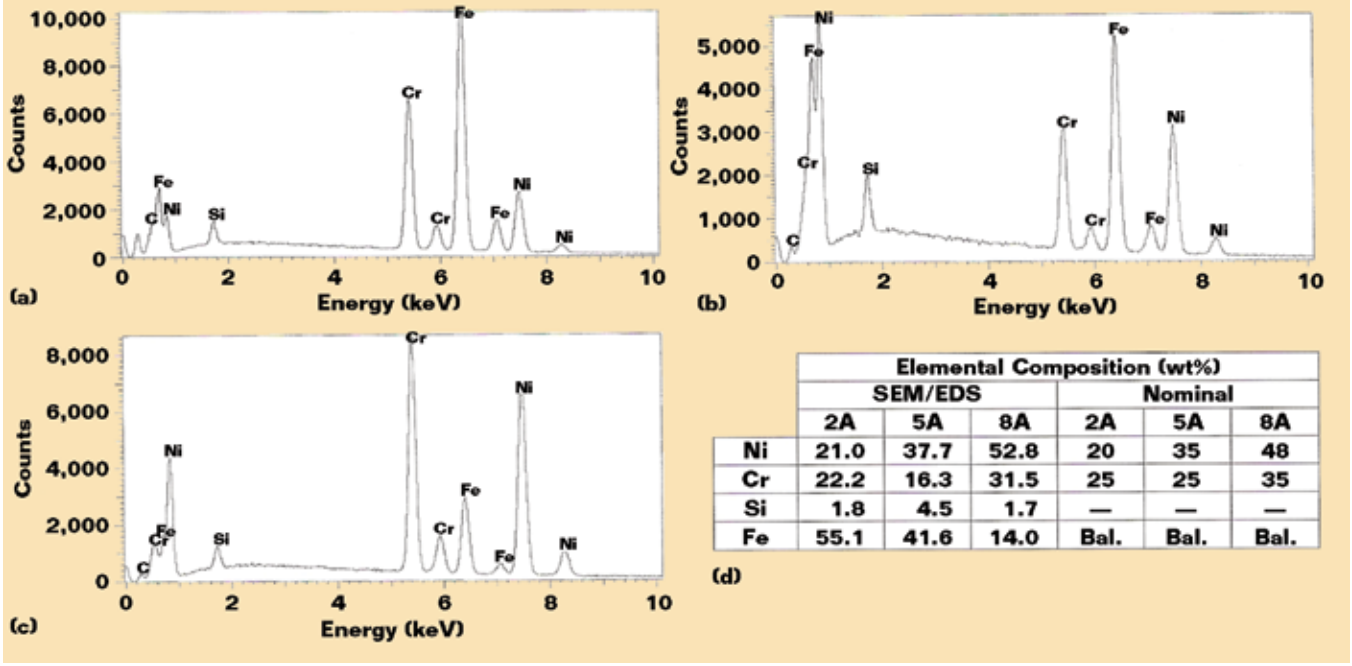

(d)

	Elemental Composition (wt%)					
	SEM/EDS			Nominal		
	2A	5A	8A	2A	5A	8A
Ni	21.0	37.7	52.8	20	35	48
Cr	22.2	16.3	31.5	25	25	35
Si	1.8	4.5	1.7	—	—	—
Fe	55.1	41.6	14.0	Bal.	Bal.	Bal.

EDS spectra derived from uncarburized austenite region for material verification of Tubes (a) 2, (b) 5, and (c) 8. (d) Results of the semi-quantitative analysis of above spectra along with the nominal compositions of the selected alloys.

FIGURE 2

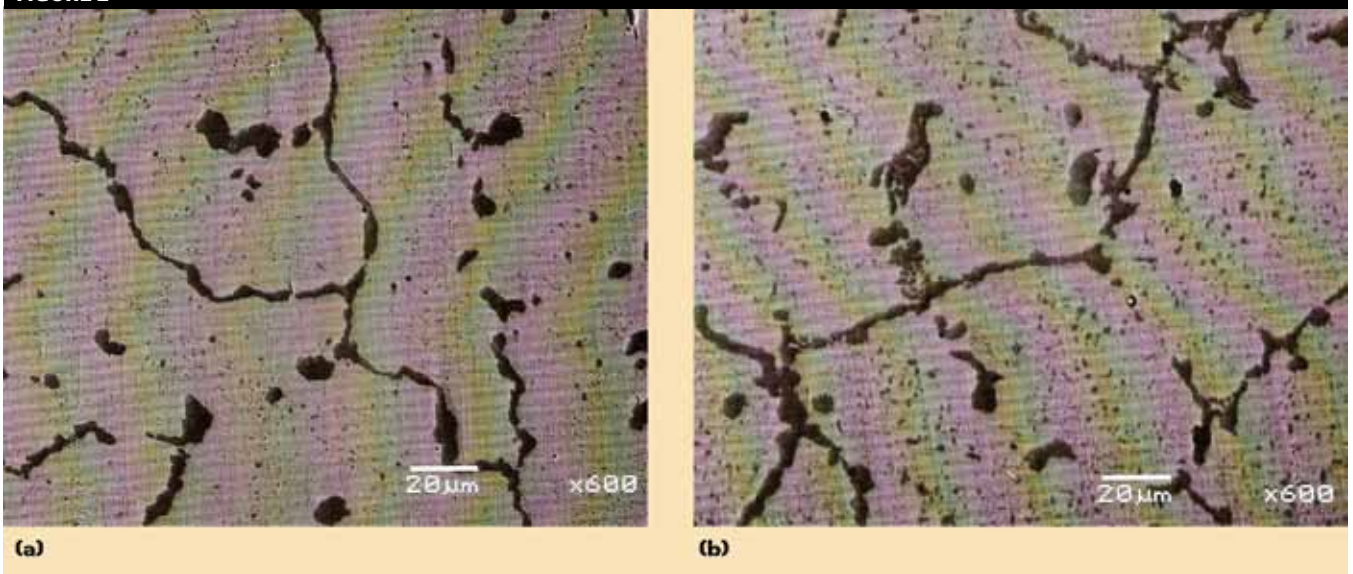

Secondary electron SEM image obtained from (a) uncarburized and (b) carburized regions of Tube 2.

to characterize the microstructural features of the scale, carburized zone, and the underlying alloy. Energy dispersive x-ray spectroscopy (EDS) combined with SEM was used to determine the elemental composition. Mechanical strength of the samples was compared using the Vickers microhardness tests.

Results

Visual Inspection

Visual inspection revealed that the tube samples, especially those with the composition of 25Cr-35Ni-Fe (Tubes 3 to 6), sagged to such a degree that they had lost their circular shape considerably. Sagging was not apparent for other tube samples. The scale formed at the surface of the tubes was adherent and there was no evidence of flaking. Also, there was no apparent cracking in tube walls.

Material Verification

EDS was used for the elemental

analyses of the tube samples. Representative EDS spectra and composition analysis for each tube material and their nominal compositions are presented in Figures 1(a) through (d).

Microstructure of Furnace Tube Materials

Microstructure of the uncarburized area of a representative furnace tube sample, particularly those designated as Tubes 1 and 2 with a nominal composition of 25Cr-20Ni-Fe (HK 40), was determined. This is presented as a secondary electron SEM image in Figure 2(a). These tube materials consist of relatively large equiaxed grains with precipitation at the grain boundaries. EDS showed that the matrix was comprised of austenite (Fe-Cr-Ni solid solution). The grain boundary consisted of a Cr-rich carbide. The presence of coarse and fine particles was also observed at the austenite matrix.

Figure 2(b) shows the microstructure of a carburized zone of the sample mentioned above. It is apparent here that the C-rich carbide precipitation present within the austenite grains are coarser in size when compared with those in the uncarburized zone.

A typical microstructure obtained from an uncarburized region of the tube material of Tubes 3 to 6 (with the nominal composition of 25Cr-35Ni Fe) is presented in the secondary electron SEM image of Figure 3(a). The carbide precipitation appears relatively coarse both at the austenite grain boundaries and within the matrix itself when compared to the uncarburized region of the tube material of Figure 2(a) (Tubes 1 and 2). This observation was corroborated by the EDS analysis where Cr concentration was determined to be 13 wt% at various regions within the austenite. The carburized region from the same sample shows a high degree of carbide precipitation at the grain boundaries and the appearance of blocky carbide particles in the matrix, as shown by the SEM image in Figure 3(b). The grain boundary precipitate was predominantly comprised of Cr, as shown by the EDS spectrum in Figure 3(c). This exhibited a continuous network. The white precipitates adjacent to the grain boundaries are Nb-rich, as shown by the EDS spectrum in Figure 3(d).

Tubes 7 to 9 (with composition of 35Cr-48Ni-Fe) have the highest Cr and Ni% composition when compared to others. Figures 4(a) and (b), respectively, show typical microstructures obtained from the uncarburized and carburized regions of the tube material. The microstructures are comprised of dark Cr-rich and white Nb-rich precipitates along with grayish precipitates. These are comparatively richer in Ni as shown in the EDS spectrum and elemental composition (Figures 4[c] and [d], respectively).

Analysis of the Scale Formed on the Tube Materials

Presented in Figure 5(a) is a typical morphology of the scale formed at the internal surface of tubes as shown in the backscattered electron SEM image. An x-ray map shown in Figure 5(b) and the various EDS spectra obtained from the region reveal that the oxide formed at the surface is Cr-rich while Fe and Ni could also be detected in the scale. In addition, Si, and Cr oxide to some extent, were detected at the austenite grain boundaries immediately beneath the alloy surface.

Effect of Carbide Precipitation

A microhardness test was performed at the carburized zone for some selected samples from Tubes 3 to 6. The tests showed the hardness to be around HV 316. The average value for the remaining tube material compositions was HV 216. Carburized zones gave higher hardness values than the uncarburized regions.

Discussion

The alloys used consisted of various percentages of elemental compositions of Cr, Ni, and Fe. The alloy of Tubes 3 to 6 consisted of 25Cr-35Ni-Fe. The Ni content was higher than in Tubes 1 and 2, which had 20Ni. Tubes 7 to 9 had higher composition percentages of Cr and Ni; that is, 35Cr-48Ni-Fe. The sagging observed in Tubes 3 to 6 is difficult to explain. It could be due to its use and/or exposure to higher furnace temperatures at the area/place of use within the furnace.

Alloy Composition

There was a difference observed in the composition between the nominal and measured values as indicated by the representative EDS spectra and composition analysis for each tube material. This observation was not, however, unexpected due to the exposure of the tubes at elevated temperature(s) in service. This exposure caused the precipitation of M-carbides (where M is Cr, Nb) within the matrix and at the grain boundaries, thus altering the starting composition of the matrix.

Carbide Precipitation

In Tubes 3 to 6, the carbide precipitation appears relatively coarse, both at the austenite grain boundaries and within the matrix. The depletion of Cr within the matrix indicates a tendency of Cr to diffuse and form Cr-rich carbides at the austenite grain boundaries and/or coarse pre-existing carbides within the austenite. Diffusion of Cr is enhanced at an elevated temperature. The higher the temperature, the greater the carburized zone and the coarser the carbide precipitates.

Scale Analysis

The previously described results obtained from the analysis of the scale formed on the furnace tube materials, as presented in Figures 5(a) and (b), indicate that the alloys were not capable of developing a protective oxide scale. This could be due, in part, to the relatively low oxygen potential in the environment typically encountered in ethylene production. The

FIGURE 3

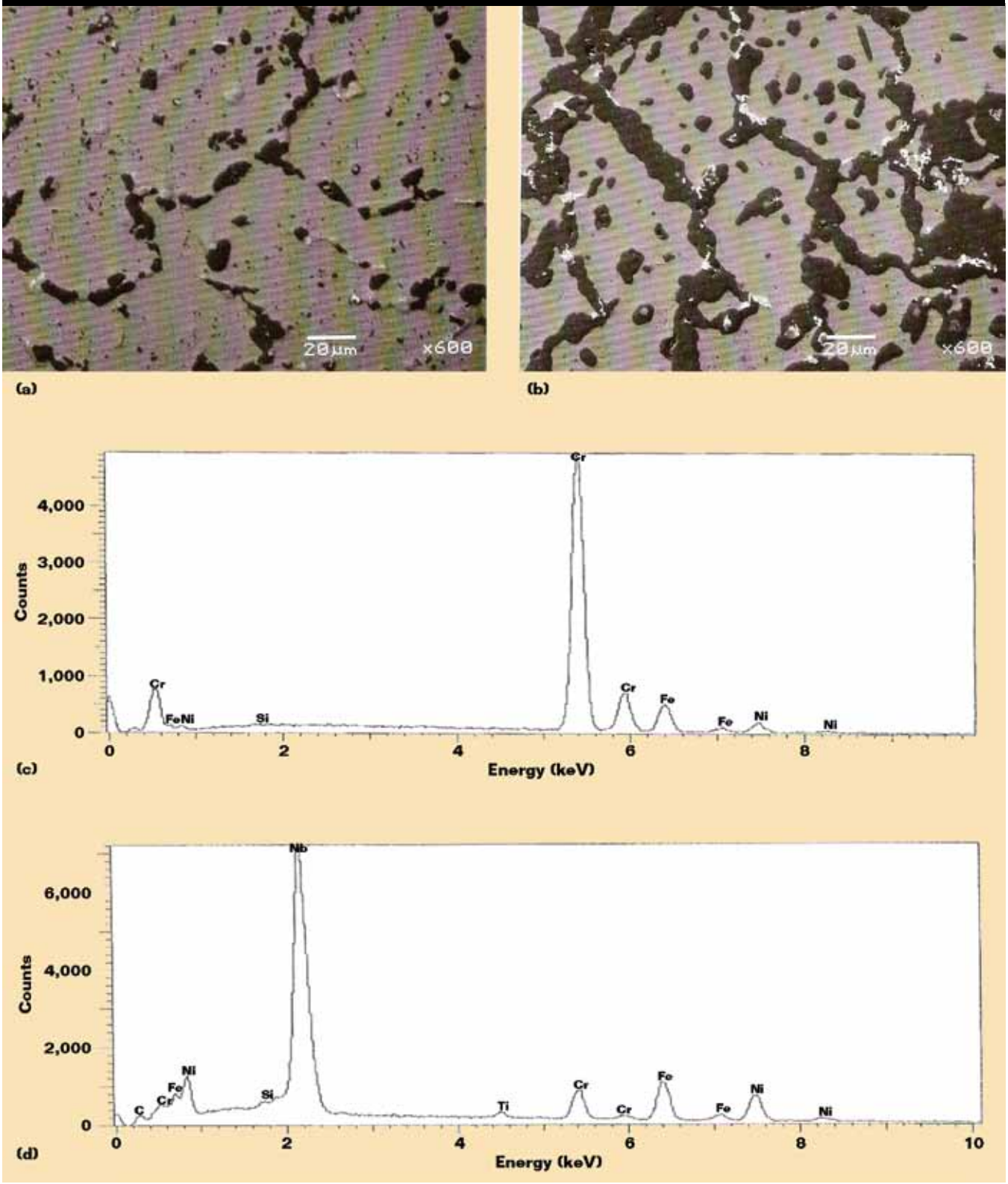

Tube 5: secondary electron SEM image of (a) uncarburized region, (b) carburized region, and EDS spectrum from (c) grain boundary precipitate showing Cr enrichment, and (d) white precipitate showing Nb enrichment.

presence of a protective oxide scale can impede carbon diffusion into the alloy and play an important role in reducing the extent of carburization attack.

Hardness

It was observed in the results obtained during the microhardness test that carburized zones of the materials gave higher hardness values (HV 316) than the uncarburized (HV 216) regions. Increased hardness at the carburized zone can be attributed to the high degree of carbide precipitation and also to carbon pick-up due to the carburizing environment. Hardness measurements combined with the microstructural observations suggest that carburization attack led to the formation of a surface-hardened layer with reduced ductility. Formation of this layer further corroborates the inability of the alloy to form a continuous protective oxide scale at its surface.

Microstructure Analysis

The typical microstructure of heat-resistant austenitic casting steels consists of austenite matrix and carbide precipitates. Varying the content of Cr and Ni in these alloys allows control of properties such as strength at elevated temperature and resistance to carburization and hot gas corrosion. Nickel imparts increased resistance to carburization attack, thermal shock, and thermal fatigue; while chromium provides increased corrosion and oxidation resistance.[5]

In the carburized region of the steel alloy tube material samples (Tubes 3 to 6), the white precipitates adjacent to the grain boundaries are Nb-rich, as shown by the EDS spectrum in Figure 3(d). Relatively small additions of Nb to heat-resistant castings can increase their resistance to thermal shock. Furthermore, Nb acts as a carbide stabilizer by forming MC-type carbides, which cause massive carbide precipitation at the grain boundaries.

Fine dispersion of carbides in the austenite matrix increases high temperature strength considerably. Rapid cooling from a temperature near the melting point leads to super saturation of carbon. Subsequent reheating (e.g., during service) will cause carbide precipitation. The lower the reheating temperature, the finer the precipitated carbides. Finer dispersion of carbides increases creep strength of the alloy. Exposure to a high temperature that leads to coarsening, agglomeration, and spherodizing of carbides, however, reduces their effectiveness as a source of strength. In addition, slow cooling from a high-temperature range will cause carbide precipitation at the austenite grain boundaries. Continuous networks of carbides at the grain boundaries are undesirable since they embrittle the alloy. The size of the carbides can be useful in indicating if the alloy has been exposed to an excessive temperature in service.

These observations suggest that the alloy had been exposed to an excessively high temperature during service.

All the furnace tubes examined showed carburization attack. Tubes 3 to 6 showed the most severe degradation of all the furnace tube samples studied in this investigation. The average depth of carburized zones in Tubes 3 to 6 was 58% of the total wall thickness as compared to 22% for Tubes 1 and 2 and 26% for Tubes 7 to 9.[6] Also, visual examination revealed that Tubes 3 to 6 were clearly sagged and significant plastic deformation occurred during service. This phenomenon was also evidenced by the SEM/EDS examination where the microstructures of these tubes showed relatively coarse blocky carbides within the austenite matrix and continuous carbide networks at the grain boundaries.

These observations suggest that the alloy had been exposed to an excessively high temperature during service. The hardness of the carburized zone was also found to be higher in Tubes 3 to 6 compared to the other tube material. This observation indicates higher precipitation and carbon pick-up by the alloy. Deposition of coke at the inner pipe wall also promoted carbon deposition and precipitation of secondary carbides within the alloy matrix.

Conclusions

From the experimental data, all the tube steel alloy materials investigated underwent carburization attack from exposure to excessively high temperatures during service.

The carburization attack was most severe in the Tubes 3 to 6. It is not possible, however, to know the specific reason for these tubes to show such a magnitude of carburization and loss of strength. There was no information about the plant process temperature, pressure, length of exposure, expected service life, operating medium, location, and orientation of tubes within the furnace.

It is recommended that the furnace temperature be closely controlled to avoid overheating during ethylene production as well as decoking.

Acknowledgments

The author acknowledges the opportunity provided by the Center for Engineering Research, The Research Institute, King Fahd University of Petroleum and Minerals, Dhahran, KSA, and the Saudi Basic Industries (SABIC) to undertake this investigation. The author also appreciates the contribution of

FIGURE 4

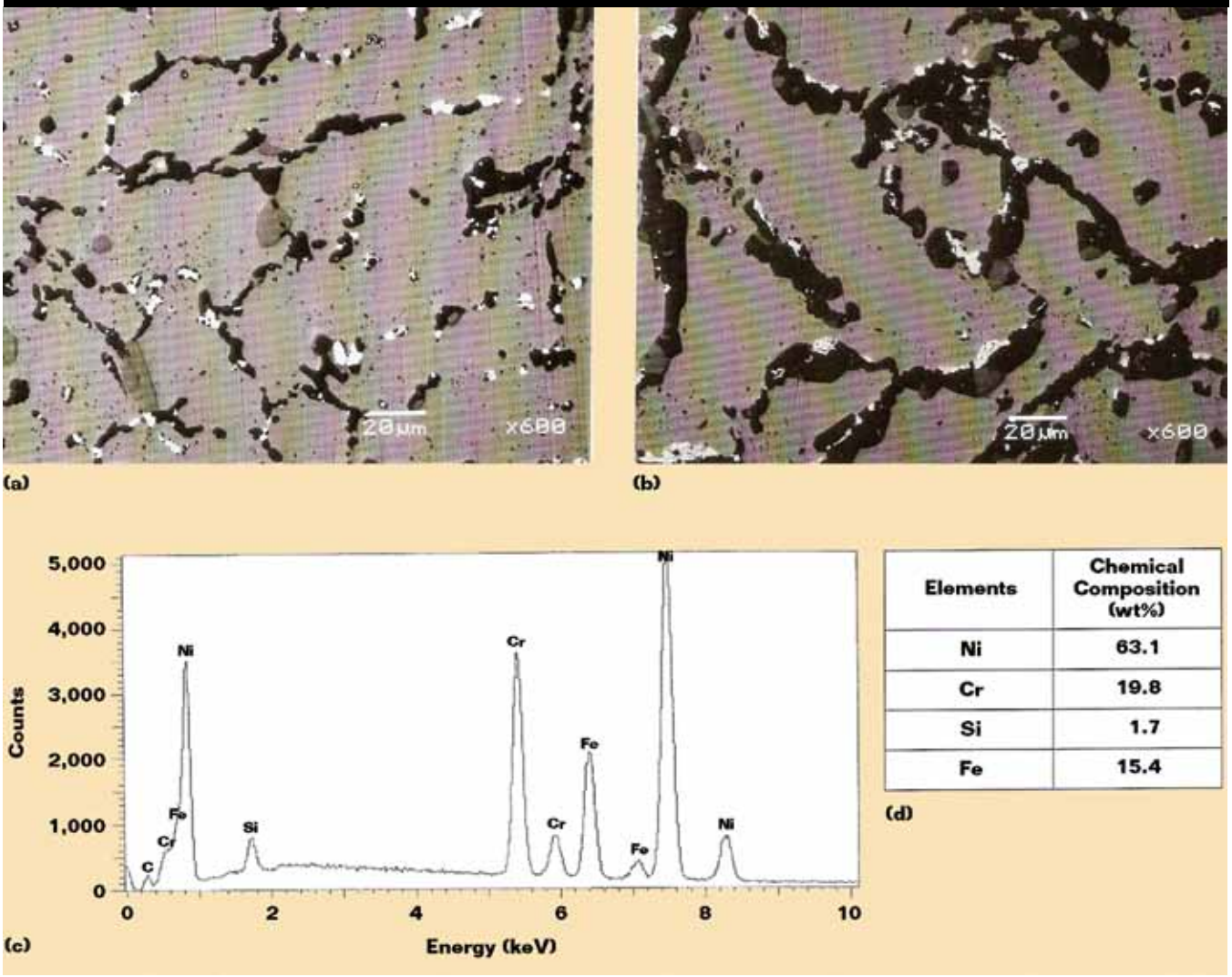

Elements	Chemical Composition (wt%)
Ni	63.1
Cr	19.8
Si	1.7
Fe	15.4

Tube 8: secondary electron SEM image of (a) uncarburized region, (b) carburized region, and EDS spectrum from (c) light gray precipitates showing a large peak of Ni, and (d) elemental composition derived from spectrum.

A.I. Mohammed (for SEM/EDS) and A. Ul-Hamid (technical report writing) and further acknowledges the provision made available by the Covenant University, Canaan Land, Ota, Nigeria, for the writing of this paper.

References

1 V. Tari, A. Najafizadeh, M.H. Aghaei, M.A. Mazloumi, *Failure Analysis and Prevention J.* 9, 4, 8 (2009): pp. 316-322.

2 A. Ul-Hamid, H. Tawancy, A.I. Mohammed, S.S. Al Jaroudi, N.M. Abbas, *J. of Failure Analysis and Prevention* 5, 4, 8 (2005): pp. 54-61.

3 Y. Nishiyama, N. Otsuka, T. Nishizawa, "Carburization Resistance of Austenitic Alloys in CH_4-CO_2-H_2 Gas Mixtures at Elevated Temperatures," *Corrosion* 59, 08 (2003): pp. 688-700.

4 B.S. Terry, J. Wright, D.J. Hall, *Corros. Sci.* 29, 6 (1989): pp. 717-734.

5 "Properties and Selection of Metals," *ASM Metals Handbook*, vol. 1, 8th ed. (Materials Park, OH: ASM International, 1977).

6 C.A. Loto, "Carburization Tests on Ethylene Furnace Tube Samples," Research Institute, KFUPM Report, MC-2000-1-13, July 2001.

CLEOPHAS AKINTOYE LOTO is a professor of mechanical/metallurgical engineering at Tshwane University of Technology, Dept. of Chemical and Metallurgical Engineering, Private Bag X680, Pretoria 0001, South Africa, e-mail: lotoca@tut.ac.za. He has worked at universities for 27 years, serving as department head several times. He has visited universities in different countries. A NACE International member since 1989, Loto has M.Sc., Ph.D., and C.Eng. degrees. MP

Continued on page @@

Continued from page @@

FIGURE 5

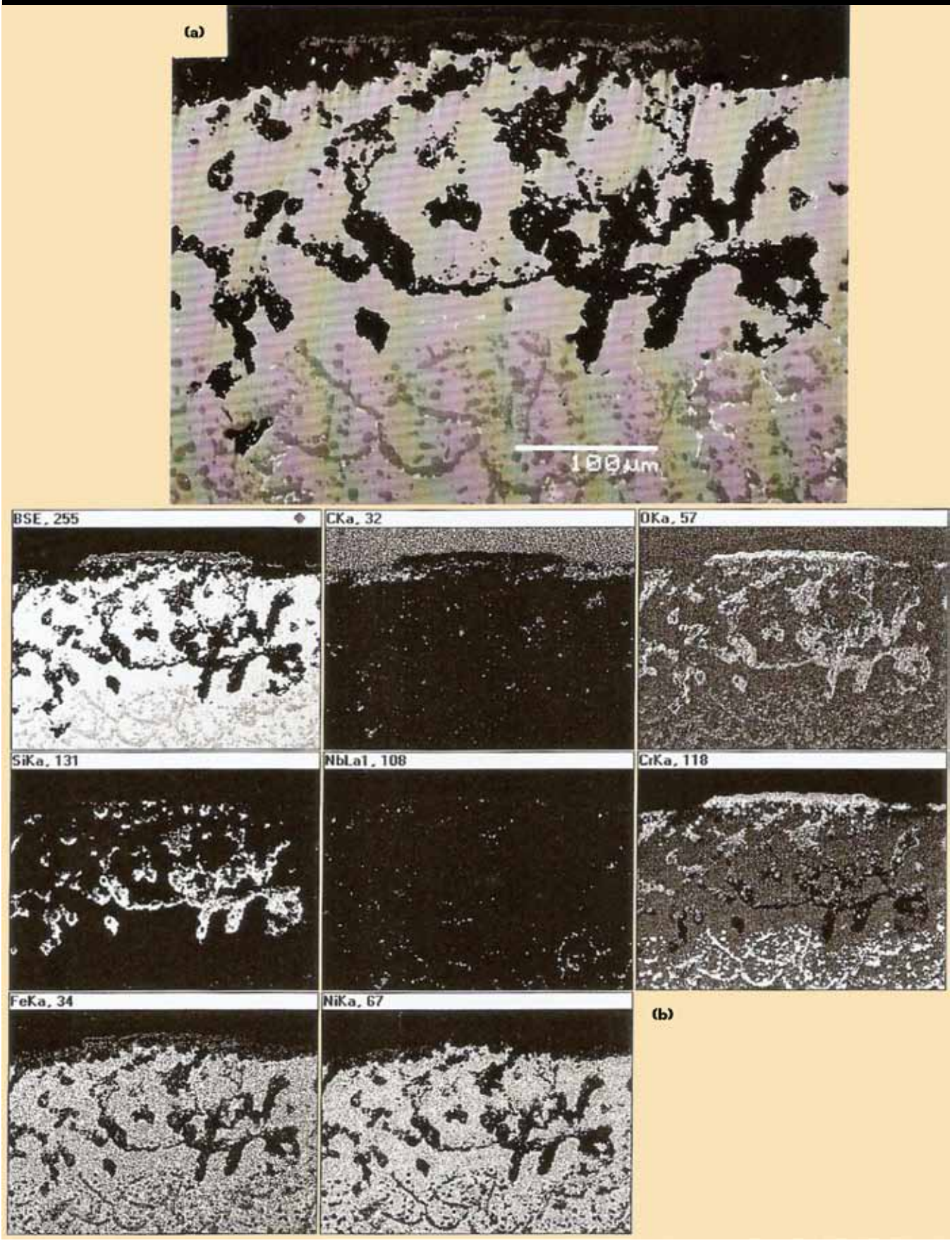

(a) Backscattered electron SEM image showing the typical morphology of scale formed at the internal surface of all tube materials and (b) an x-ray map showing the distribution of various elements within the scale and the underlying region.